NEOPLASIA
www.neoplasia.com
Volume 10 Number 6 June 2008 pp. 534–541 534

PIK3CA Mutation in Colorectal Cancer: Relationship with Genetic and Epigenetic Alterations[1]

Katsuhiko Nosho[*,2], Takako Kawasaki[*,2], Mutsuko Ohnishi[*], Yuko Suemoto[*], Gregory J. Kirkner[†], Dimity Zepf[‡], Liying Yan[§], Janina A. Longtine[‡], Charles S. Fuchs[*,†] and Shuji Ogino[*,‡,¶]

*Department of Medical Oncology, Dana-Farber Cancer Institute, Boston, MA 02115 USA; †Channing Laboratory, Department of Medicine, Brigham and Women's Hospital, and Harvard Medical School, Boston, MA 02115 USA; ‡Department of Pathology, Brigham and Women's Hospital, and Harvard Medical School, Boston, MA 02115 USA; §EpigenDx, Worcester, MA 01606 USA; ¶Department of Epidemiology, Harvard School of Public Health, Boston, MA 02115 USA

Abstract

Somatic *PIK3CA* mutations are often present in colorectal cancer. Mutant *PIK3CA* activates AKT signaling, which up-regulates fatty acid synthase (*FASN*). Microsatellite instability (MSI) and CpG island methylator phenotype (CIMP) are important molecular classifiers in colorectal cancer. However, the relationship between *PIK3CA* mutation, MSI and CIMP remains uncertain. Using Pyrosequencing technology, we detected *PIK3CA* mutations in 91 (15%) of 590 population-based colorectal cancers. To determine CIMP status, we quantified DNA methylation in eight CIMP-specific promoters [*CACNA1G*, *CDKN2A* (p16), *CRABP1*, *IGF2*, *MLH1*, *NEUROG1*, *RUNX3*, and *SOCS1*] by real-time polymerase chain reaction (MethyLight). *PIK3CA* mutation was significantly associated with mucinous tumors [$P = .0002$; odds ratio (OR) = 2.44], *KRAS* mutation ($P < .0001$; OR = 2.68), CIMP-high ($P = .03$; OR = 2.08), phospho–ribosomal protein S6 expression ($P = .002$; OR = 2.19), and *FASN* expression ($P = .02$; OR = 1.85) and inversely with p53 expression ($P = .01$; OR = 0.54) and β-catenin (CTNNB1) alteration ($P = .004$; OR = 0.43). In addition, *PIK3CA* G-to-A mutations were associated with MGMT loss ($P = .001$; OR = 3.24) but not with *MGMT* promoter methylation. In conclusion, *PIK3CA* mutation is significantly associated with other key molecular events in colorectal cancer, and MGMT loss likely contributes to the development of *PIK3CA* G>A mutation. In addition, Pyrosequencing is useful in detecting *PIK3CA* mutation in archival paraffin tumor tissue. *PIK3CA* mutational data further emphasize heterogeneity of colorectal cancer at the molecular level.

Neoplasia (2008) 10, 534–541

Abbreviations: CI, confidence interval; CIMP, CpG island methylator phenotype; FASN, fatty acid synthase; LOH, loss of heterozygosity; MSI, microsatellite instability; MSS, microsatellite stable; OR, odds ratio; PI3K, phosphatidylinositol 3-kinase; *PIK3CA*, phosphoinositide-3-kinase, catalytic, alpha polypeptide; RPS6, ribosomal protein S6

Address all correspondence to: Shuji Ogino, MD, PhD, Center for Molecular Oncologic Pathology, Dana-Farber Cancer Institute, Brigham and Women's Hospital, Harvard Medical School, 44 Binney St, Room JF-215C, Boston, MA 02115. E-mail: shuji_ogino@dfci.harvard.edu

[1]This work was supported by the National Institutes of Health grants P01 CA87969, P01 CA55075, P50 CA127003, and K07 CA122826 (to S. O.), and in part by grants from the Bennett Family Fund and the Entertainment Industry Foundation (EIF) through the EIF National Colorectal Cancer Research Alliance. M. O. was supported by Japanese Foundation for Multidisciplinary Treatment of Cancer. These funding sponsors had no role or involvement in the study design, the collection, analysis, and interpretation of data, or in writing and submission of the manuscript.

[2]These authors equally contributed to this work.

Received 27 February 2008; Revised 27 March 2008; Accepted 29 March 2008

DOI 10.1593/neo.08336

Introduction

The phosphoinositide-3-kinase, catalytic, alpha polypeptide (*PIK3CA*) gene encodes the catalytic subunit p110 alpha of phosphatidylinositol 3-kinase (PI3K) belonging to class 1A of PI3Ks [1,2]. Phosphatidylinositol 3-kinase interacts with phosphatidylinositol-3-phosphate at the membrane and catalyzes the phosphorylation of AKT, which activates the downstream signaling pathway [1]. Mutant *PIK3CA* stimulates the AKT pathway and promotes cell growth in various cancers [3]. In addition, the AKT signaling pathway regulates fatty acid synthase (FASN) expression [4–6] that has been implicated in the development of cancers including colorectal cancer [7].

PIK3CA mutations have been described in 10% to 30% of colorectal cancers [8–15] and have been associated with microsatellite instability (MSI) [11]. Most sporadic MSI-high colorectal cancers arise through *MLH1* promoter methylation due to the CpG island methylator phenotype (CIMP) [16–19]. MSI and CIMP reflect global genomic and epigenomic aberrations, respectively, in tumor cells and largely determine clinical, pathologic, and molecular characteristics of colorectal cancer [20]. Thus, a molecular classification based on MSI and CIMP status is increasingly important [20,21]. However, the relationship between *PIK3CA* mutation and CIMP remains uncertain.

In this study, using Pyrosequencing technology and a large number of population-based colorectal cancers, we examined *PIK3CA* mutation in relation to MSI, CIMP, and other relevant molecular events. We also examined whether *PIK3CA* G>A mutation could be attributed to MGMT loss and subsequent DNA repair defect. Pyrosequencing has been shown to be useful to detect mutant alleles of low abundance as observed in solid tumor specimens [22].

Materials and Methods

Study Group

We used the databases of two large prospective cohort studies: the Nurses' Health Study (N = 121,700 women followed since 1976) [23] and the Health Professionals Follow-up Study (N = 51,500 men followed since 1986) [24]. Informed consent was obtained from participants on inclusion in the cohorts. A subset of the cohort participants developed colorectal cancers during prospective follow-up. Previous studies on the Nurses' Health Study and Health Professionals Follow-up Study have described baseline characteristics of cohort participants and incident colorectal cancer cases and confirmed that our colorectal cancers were a good representative of a population-based sample [23,24]. We collected paraffin-embedded tissue blocks from hospitals where cohort participants with colorectal cancers had undergone resections of primary tumors. On the basis of availability of tissue, a total of 590 colorectal cancers (272 from the men's cohort and 318 from the women's cohort) were included in this study. Among our cohort studies, there was no significant difference in demographic features between cases with tissue available and those without available tissue [25]. Hematoxylin and eosin–stained tissue sections were examined by a pathologist (S. O.) unaware of clinical and other laboratory data [26]. Although many of the cases have been previously characterized for status of CIMP, MSI, *KRAS*, *BRAF*, and p53 [26], we have not examined *PIK3CA* mutation or ribosomal protein S6 (RPS6) in our specimens. Tissue collection and analyses were approved by the Brigham and Women's Hospital and Harvard School of Public Health Institutional Review Boards.

Genomic DNA Extraction, Whole Genome Amplification, and KRAS *and* BRAF *Sequencing*

Genomic DNA was extracted from dissected tumor tissue sections using QIAmp DNA Mini Kit (Qiagen, Valencia, CA) [22]. Normal DNA was obtained from colonic tissue at resection margins. Whole genome amplification (WGA) of genomic DNA was performed by polymerase chain reaction (PCR) using random 15-mer primers [22,27]. Polymerase chain reaction and Pyrosequencing were performed as previously described (*KRAS* [22] and *BRAF* [28]).

Pyrosequencing for PIK3CA *(Table 1)*

We developed Pyrosequencing assay to detect *PIK3CA* mutations, because Pyrosequencing has been shown to be applicable to paraffin-embedded tumors and more sensitive than Sanger dideoxy sequencing in *KRAS* mutation analysis [22]. The exon 9 PCR primers were: PIK3CA 9-F, 5′-biotin-AACAGCTCAAAGCAATTTCTACACG-3′; and PIK3CA 9-R, 5′-ACCTGTGACTCCATAGAAAATCTTT-3′ (Figure 1). Each PCR mix contained the forward and reverse primers (each 10 μM), 12.5 mM each of dNTP Mix with dUTP, 0.0175 U of AmpErase (Uracil-N glycosylase; Applied Biosystems, Forster City, CA), 3 mM of $MgCl_2$, 1× PCR buffer, 1.5 U of AmpliTaq Gold (Applied Biosystems), and 3 μl of template WGA product in a total volume of 35 μl. The exon 20 PCR primers were: PIK3CA 20-F, 5′-biotin-CAAGAGGCTTTGGAGTATTTCA-3′; and PIK3CA 20-R, 5′-CAATCCATTTTTGTTGTCCA-3′. Each PCR mix contained the forward and reverse primers (each 10 μM), 12.5 mM each of dNTP Mix with dUTP, 0.02 U of AmpErase, 3 mM of $MgCl_2$, 1× PCR buffer, 1 U of AmpliTaq Gold, and 2 μl of template WGA product in a total volume of 25 μl. Polymerase chain reaction conditions were as follows: initial denaturing at 95°C for 5 minutes; 50 cycles of 94°C for 20 seconds, 50°C for 20 seconds, and 74°C for 40 seconds; and final extension at 72°C for 1 minute. The PCR products were electrophoresed in an agarose gel to confirm successful amplifications of the 81- (exon 9) and 74-bp (exon 20) products. The PCR products (each 10 μl) were sequenced by Pyrosequencing PSQ96 HS System (Biotage, Uppsala, Sweden) according to manufacturer's instructions.

To increase sensitivity, we designed three different Pyrosequencing primers for *PIK3CA* exon 9, using the ADSW software (Biotage) (Figure 1). The use of three sequencing primers served as a quality control measure, because exon 9 mutations (except for nucleotides 1634–1636) could be detected by at least two primers. Representative Pyrograms of wild type and mutant exon 9 sequence by these primers are shown in Figure 2. The primer *PIK3CA* 9-RS1

Table 1. *PIK3CA* Mutations in Colorectal Cancer.

Exon	Domain	Nucleotide Change*	Codon Change*	Number of Cases
9	Helical	c.1624G>A	p.E542K	18†
9	Helical	c.1633G>A	p.E545K	30†
9	Helical	c.1634A>G	p.E545G	1
9	Helical	c.1636C>A	p.Q546K	7
20	Kinase	c.3129G>T	p.M1043I	8
20	Kinase	c.3133G>A	p.D1045N	1
20	Kinase	c.3136G>A	p.A1046T	2
20	Kinase	c.3139C>T	p.H1047Y	3
20	Kinase	c.3140A>G	p.H1047R	18
20	Kinase	c.3140A>T	p.H1047L	5

*Nomenclature of mutation follows the recommendations by the Human Genome Variation Society (http://www.hgvs.org/mutnomen/).

†Two cases had both c.1624G>A and c.1633G>A mutations.

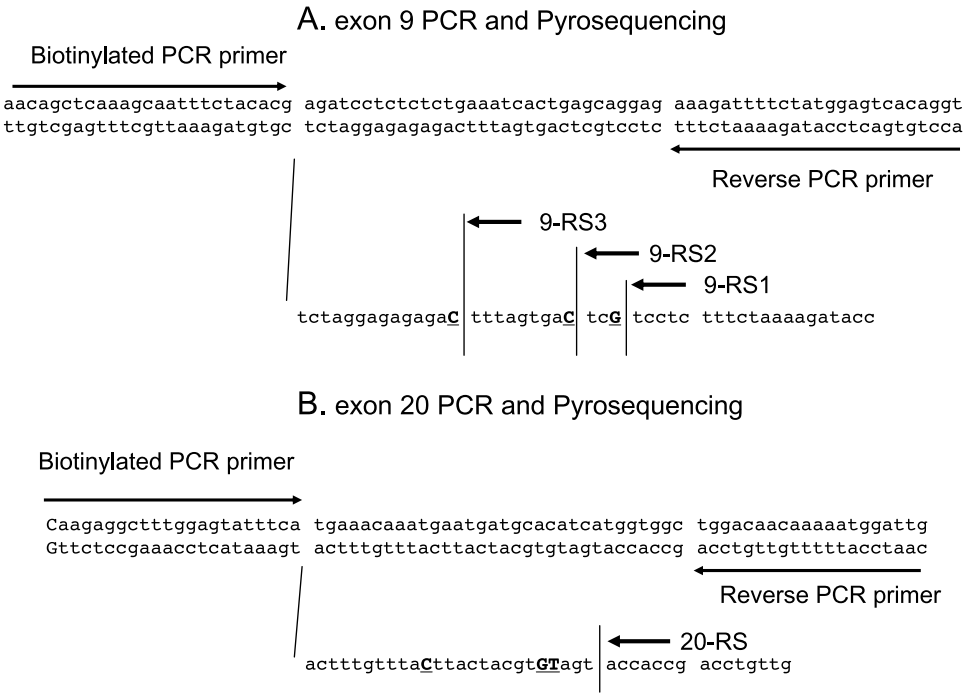

Figure 1. *PIK3CA* Pyrosequencing assay design. (A) The exon 9 PCR products were sequenced by the three different Pyrosequencing primers (9-RS1, 9-RS2, and 9-RS3). Nucleotide positions of the hot spot mutations are underlined and in bold capitals. (B) The exon 20 PCR products were sequenced by the Pyrosequencing primer (20-RS). Nucleotide positions of the hot spot mutations are underlined and in bold capitals.

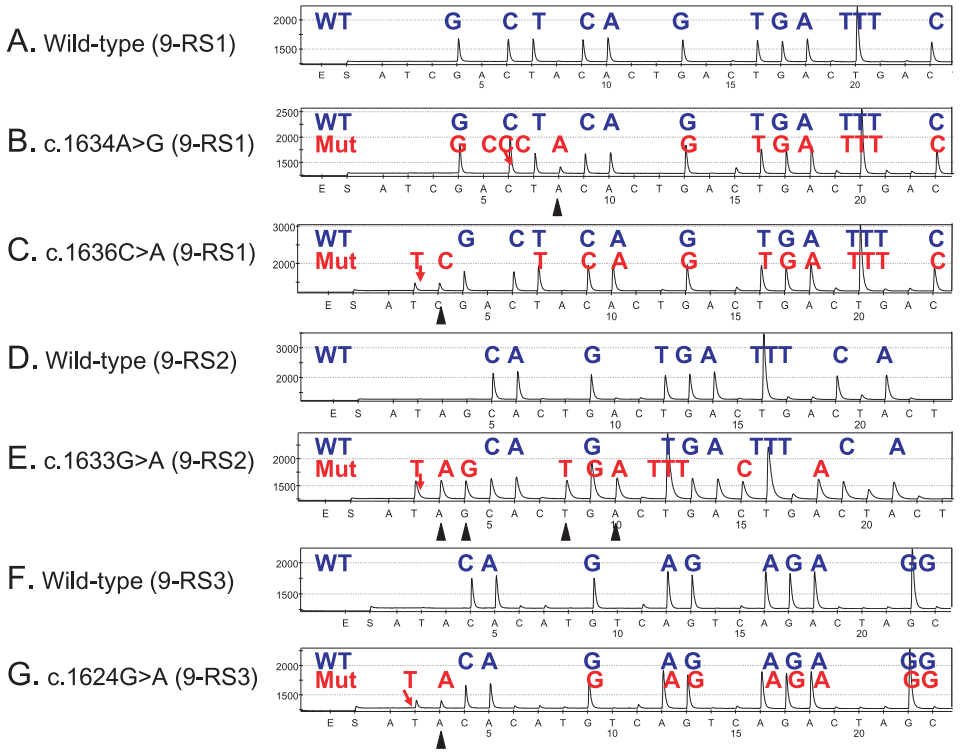

Figure 2. *PIK3CA* exon 9 Pyrograms (antisense strand). (A) Wild type exon 9 by the 9-RS1 primer. (B) The c.1634A>G mutation (arrow) causes a shift in reading frame and results in a new peak at A (arrowhead), which serves as quality assurance. (C) The c.1636C>A mutation (arrow) causes a shift in reading frame and results in a new peak at C (arrowhead), which serves as quality assurance. (D) Wild type exon 9 by the 9-RS2 primer. (E) The c.1633G>A mutation (arrow) causes a shift in reading frame and results in new peaks (arrowheads), which serves as quality assurance. (F) Wild type exon 9 by the 9-RS3 primer. (G) The c.1624G>A mutation (arrow) causes a shift in reading frame and results in a new peak at A (arrowhead), which serves as quality assurance. *Mut* indicates mutant; *WT*, wild type.

(5′-CCATAGAAAATCTTTCTCCT-3′; nucleotide dispensation order, ATCGACTACACTGACTGACTGACTGACTGACTGACT-G) could detect the c.1634A>G and c.1636C>A mutations (Figure 2, *B* and *C*). The primer *PIK3CA* 9-RS2 (5′-TAGAAAATCTT-TCTCCTGCT-3′; nucleotide dispensation order, ATAGCACT-GACTGACTGACTACTGACTGACTGACTG) could detect the most common mutations [c.1633G>A (Figure 2*E*) and c.1624G>A]. The primer *PIK3CA* 9-RS3 (5′-TTCTCCTTGCTTCAGTGATTT-3′; nucleotide dispensation order, ATACACATGTCAGTCAGAC-TAGCTAGCTAGCTAG) was particularly sensitive to detect c.1624G>A mutation (Figure 2*G*). For *PIK3CA* exon 20, we designed the primer *PIK3CA* 20-RS (5′-GTTGTCCAGCCACCA-3′; nucleotide dispen-sation order, CTGACGATACTGTGCATCATATGCATGCATG-CATGCATGC) to detect various exon 20 mutations (c.3140A>G, c.3129G>T, etc.; Figure 3).

Nucleotide dispensation orders were designed so that, if any of the common mutations was present, it caused a shift in reading frame and resulted in additional new peak(s) (indicated by *arrowheads* in Figures 2 and 3) following the mutated nucleotide. This feature, which was absent in Sanger (dideoxy) sequencing, could serve as quality assurance and confirmation of the presence of the mutations.

Microsatellite Instability and 18q Loss of Heterozygosity (LOH)

Microsatellite instability analysis was performed as previously described [29] with D2S123, D5S346, D17S250, BAT25, and BAT26 [30] in addition to BAT40, D18S55, D18S56, D18S67 and D18S487 (i.e., 10-marker panel). MSI-high was defined as the presence of instability in ≥30% of markers, MSI-low as instability in <30% of markers, and microsatellite stable (MSS) as no unstable marker.

Loss of heterozygosity at each locus in 18q was defined as 40% or greater reduction of one of two allele peaks in tumor DNA relative to normal DNA in two duplicated runs [29]. Overall 18q LOH(+) was strictly defined as the presence of LOH in at least two 18q markers, and 18q LOH(–) as the presence of at least two informative 18q makers without evidence of LOH.

Real-time PCR (MethyLight) for Quantitative DNA Methylation Analysis

Sodium bisulfite modification and quantitative real-time PCR (MethyLight [31]) were validated and performed as previously described [32,33]. We quantified methylation in *MGMT* and eight CIMP-specific promoters (*CACNA1G*, *CDKN2A* (p16), *CRABP1*, *IGF2*, *MLH1*, *NEUROG1*, *RUNX3*, and *SOCS1*) [17,18,26]; the latter eight were selected from screening of 195 CpG islands [17,18] and constituted a CIMP diagnostic panel [26]. The PCR condition was initial denaturation at 95°C for 10 minutes followed by 45 cycles of 95°C for 15 seconds and 60°C for 1 minute.

CIMP-high was defined as the presence of ≥6 of 8 methylated promoters, CIMP-low as the presence of 1/8 to 5/8 methylated promoters, and CIMP-0 as the absence (0/8) of methylated promoters, according to the previously established criteria [26].

Tissue Microarrays and Immunohistochemistry for p53, MGMT, FASN, β-Catenin, and Phospho-RPS6

Tissue microarrays were constructed as previously described [34]. For phospho-RPS6 immunohistochemistry, antigen retrieval was performed; deparaffinized tissue sections were treated by a microwave for 15 minutes in citrate buffer (BioGenex, San Ramon, CA). Tissue sections were incubated with 3% H_2O_2 (10 minutes), then incubated with 10% normal goat serum (Vector Laboratories, Burlingame, CA) in phosphate-buffered saline (10 minutes). Primary antibody against phospho-RPS6 (Ser240/244, catalogue #2215; Cell Signaling, Danvers,

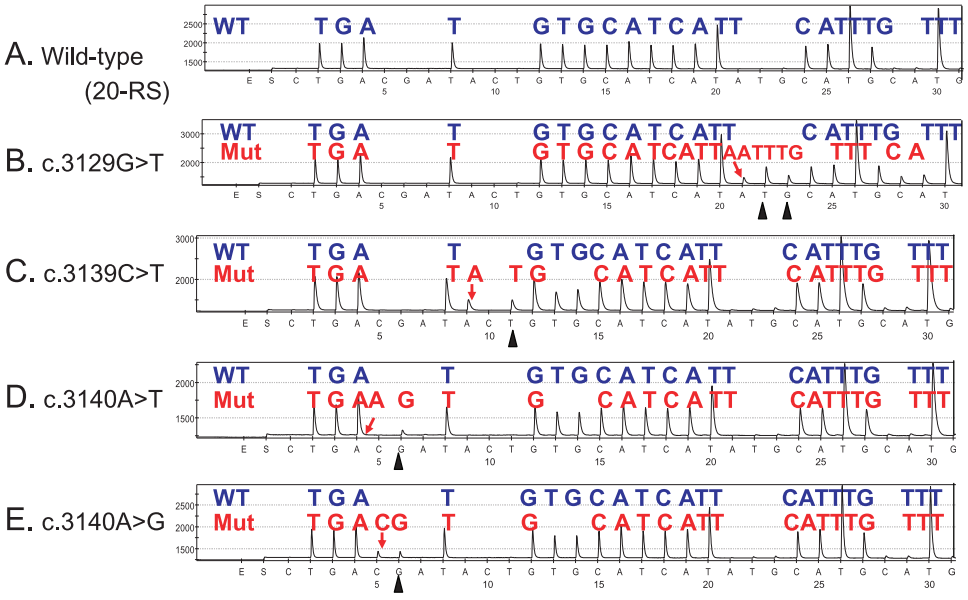

Figure 3. *PIK3CA* exon 20 Pyrograms (antisense strand). (A) Wild type exon 20. (B) The c.3129G>T mutation (arrow) causes a shift in reading frame and results in new peaks at T and G (arrowheads), which serves as quality assurance. (C) The c.3139C>T mutation (arrow) causes a shift in reading frame and results in a new peak at T (arrowhead), which serves as quality assurance. (D) The c.3140A>T mutation (arrow) causes a shift in reading frame and results in a new peak at G (arrowhead), which serves as quality assurance. (E) The c.3140A>G mutation (arrow) causes a shift in reading frame and results in a new peak at G (arrowhead), which serves as quality assurance. *Mut* indicates mutant; *WT*, wild type.

MA) (dilution 1:100) was applied overnight at 4°C. Secondary antibody (Vectorstain Elite ABC Rabbit kit; Vector Laboratories) (30 minutes), and then ABC conjugates were applied (30 minutes). Sections were visualized by diaminobenzidine (5 minutes) and methyl-green counterstain. Phospho-RPS6 positivity was defined as tumor cells with moderate/strong cytoplasmic staining.

Other immunohistochemical assays were performed as previously described (p53 [34], MGMT [35], FASN [29], and β-catenin [36]). β-Catenin activation score (0 to 5) [36] was calculated as previously described by Jass et al. [37]. Appropriate positive and negative controls were included in each run of immunohistochemistry. All immunohistochemically stained slides were interpreted by a pathologist (S. O., except for β-catenin and RPS6 by K. N.) unaware of clinical and other laboratory data.

Statistical Analysis

For categorical data, χ^2 test (or Fisher's exact test when any expected cell count is <5) was performed, and 95% confidence interval (CI) of odds ratio (OR) was computed using SAS program (version 9.1; SAS Institute, Cary, NC). All *P* values were two-sided, and statistical significance was set at $P \leq .05$.

Results

PIK3CA *Mutation in Colorectal Cancer*

We examined *PIK3CA* exons 9 and 20 by Pyrosequencing (Figures 1–3) and detected mutations in 91 (15%) of 590 colorectal cancers. Pyrosequencing technology has been shown to be applicable to paraffin-embedded tumor tissue and more sensitive than Sanger (dideoxy) sequencing [22]. A distribution of various *PIK3CA* mutations detected in our colorectal cancers (Table 1) was essentially in agreement with the previous studies [8–13]. The most common mutation was the c.1633G>A (p.E545K) mutation present in 30 tumors, followed by c.1624G>A (p.E542K) and c.3140A>G (p.H1047R) (each present in 18 tumors).

Table 2 summarizes the frequencies of *PIK3CA* mutation. *PIK3CA* mutation was more common in well-differentiated tumors (25% = 44/179) than in moderately/poorly differentiated tumors (12% = 47/407, $P < .0001$). *PIK3CA* mutation was more frequent in mucinous tumors (23% = 44/189, $P = .0002$) than nonmucinous tumors (11% = 36/325). *PIK3CA* mutation was not significantly correlated with age, sex, tumor location, stage, or signet ring cells.

PIK3CA *Mutation Is Associated with CIMP-High and* KRAS *Mutation*

Table 3 shows the frequencies of *PIK3CA* mutation according to the molecular alterations in colorectal cancer. We determined the CIMP status using MethyLight assays on a panel of eight CIMP-specific promoters (*CACNA1G*, *CDKN2A*, *CRABP1*, *IGF2*, *MLH1*, *NEUROG1*, *RUNX3*, and *SOCS1*) [18,26]. CIMP-high tumors (with ≥6/8 methylated promoters) demonstrated a higher frequency of *PIK3CA* mutation (22% = 17/78, $P = .03$) than CIMP-0 tumors (12% = 33/279). When tumors were classified according to combined MSI and CIMP status, compared with the non–MSI-high CIMP-low/0 subtype, subtypes with CIMP-high or MSI-high showed higher frequencies of *PIK3CA* mutation, although differences were not statistically significant.

PIK3CA mutation was more common in *KRAS*-mutated tumors (24% = 53/223, $P < .0001$) than *KRAS* wild type tumors (10% = 38/365). In contrast, no significant relationship was found between *PIK3CA* and *BRAF* mutations.

Table 2. Frequency of *PIK3CA* Mutation in Colorectal Cancer.

Clinical/Pathologic Feature	*n*	*PIK3CA* Mutation [*n* (%)]	OR (95% CI)	*P*
All cases, *N*	590	91 (15)		
Gender				
Men	272	43 (16)	1	
Women	318	48 (15)	0.95 (0.61–1.48)	
Age, yr				
<59	147	19 (13)	1	
60–69	244	37 (15)	1.20 (0.66–2.18)	
≥70	198	35 (18)	1.45 (0.79–2.65)	
Location				
Proximal	244	46 (19)	1	
Distal	324	43 (13)	0.66 (0.42–1.04)	
Tumor stage				
I	134	21 (16)	1	
II	165	28 (17)	1.10 (0.59–2.04)	
III	160	27 (17)	1.09 (0.59–2.04)	
IV	67	9 (13)	0.84 (0.36–1.94)	
Differentiation				
Well	179	44 (25)	1	Referent
Moderate/Poor	407	47 (12)	0.40 (0.25–0.63)	<.0001
Mucinous component				
Absent	325	36 (11)	1	Referent
Present (≥1%)	189	44 (23)	2.44 (1.50–3.95)	.0002
Signet ring cells				
Absent	449	67 (15)	1	
Present (≥1%)	38	6 (16)	1.07 (0.43–2.66)	

CI indicates confidence interval; *OR*, odds ratio.

Table 3. Frequency of *PIK3CA* Mutation in Colorectal Cancer According to Various Molecular Features.

Molecular Feature	*n*	PIK3CA Mutation [*n* (%)]	OR (95% CI)	*P*
MSI status				
MSS	458	65 (14%)	1	
MSI-low	52	11 (21%)	1.62 (0.79–3.32)	
MSI-high	74	15 (20%)	1.54 (0.82–2.87)	
CIMP status				
CIMP-0	279	33 (12%)	1	Referent
CIMP-low	233	41 (18%)	1.59 (0.97–2.61)	
CIMP-high	78	17 (22%)	2.08 (1.09–3.97)	.03
MSI/CIMP status				
Non–MSI-high CIMP-low/0	485	69 (14%)	1	
MSI-high CIMP-low/0	21	5 (24%)	1.88 (0.67–5.31)	
Non–MSI-high CIMP-high	25	7 (28%)	2.34 (0.94–5.82)	
MSI-high CIMP-high	53	10 (19%)	1.40 (0.67–2.92)	
KRAS mutation				
(–)	365	38 (10%)	1	Referent
(+)	223	53 (24%)	2.68 (1.70–4.23)	<.0001
BRAF mutation				
(–)	505	79 (16%)	1	
(+)	71	10 (14%)	0.88 (0.43–1.80)	
p53 expression				
(–)	327	60 (18%)	1	Referent
(+)	257	28 (11%)	0.54 (0.34–0.88)	.01
18q LOH				
(–)	148	25 (17%)	1	
(+)	168	18 (11%)	0.59 (0.31–1.13)	
β-Catenin score*				
0–2 (inactive)	321	61 (19%)	1	Referent
3–5 (active)	184	17 (9.2%)	0.43 (0.25–0.77)	.004
FASN expression				
(–)	222	24 (11%)	1	Referent
(+)	355	65 (18%)	1.85 (1.12–3.05)	.02
Phospho-RPS6				
(–)	323	41 (13%)	1	Referent
(+)	149	36 (24%)	2.19 (1.33–3.61)	.002

CI indicates confidence interval; *CIMP*, CpG island methylator phenotype; *FASN*, fatty acid synthase; *LOH*, loss of heterozygosity; *MSI*, microsatellite instability; *MSS*, microsatellite stable; *OR*, odds ratio; *RPS6*, ribosomal protein S6.
*β-Catenin score is the sum of nuclear, cytolasmic, and membrane score as described by Jass et al. [37].

PIK3CA *Mutation and Other Molecular Changes*

PIK3CA mutation was significantly associated with the expressions of phospho-RPS6 (P = .002) and FASN (P = .02) and inversely associated with p53 expression (P = .01) and β-catenin activation (P = .004; Table 3). Although *PIK3CA* mutation was more common in MSI-high (20%) and MSI-low tumors (21%) than in MSS tumors (14%), differences were not statistically significant.

PIK3CA *G>A Mutation Is Associated with* MGMT *Loss*

The G-to-A substitution was the most common nucleotide change in *PIK3CA* exons 9 and 20 (Table 1). Considering the known association between *MGMT* methylation/silencing and G>A mutations in *KRAS* and *TP53* [38,39], we examined whether there was a relation between *MGMT* methylation/silencing and *PIK3CA* G>A mutation (Figure 4). *PIK3CA* G>A mutation was significantly more common in tumors with MGMT loss [14% = 22/158, P = .001; OR = 3.24, 95% CI 1.55–6.74] than MGMT-expressing tumors (4.8% = 12/252). In contrast, *PIK3CA* non–G>A mutation was not significantly associated with MGMT loss. *PIK3CA* G>A mutation was not significantly associated with *MGMT* promoter methylation.

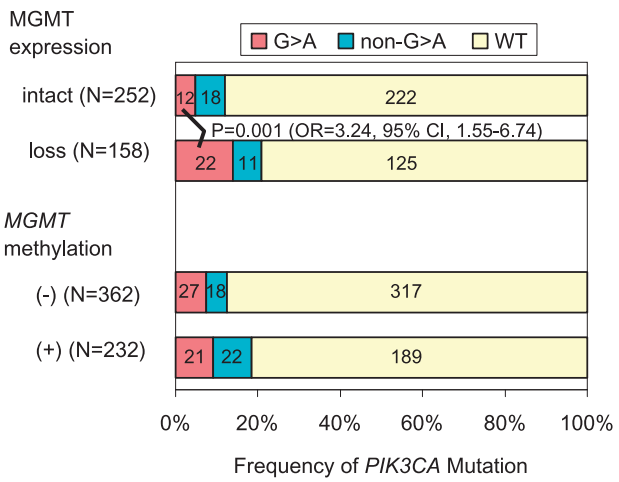

Figure 4. Frequencies of *PIK3CA* G>A and non–G>A mutations according to *MGMT* status. *PIK3CA* G>A mutation was significantly associated with MGMT loss (P = .001). No significant association was found between *PIK3CA* non–G>A mutation and *MGMT* loss. *CI* indicates confidence interval; *OR*, odds ratio; *WT*, wild type.

Discussion

We conducted this study to examine the relationship between *PIK3CA* mutation and various genetic and epigenetic alterations in colorectal cancer. The PI3K-AKT pathway is important in the development of various cancers [1,2], and activating mutations in the *PIK3CA* gene have been identified in colorectal cancer [8–15]. We have demonstrated that *PIK3CA* mutation is significantly associated with the CIMP, *KRAS* mutation, and FASN expression in colorectal cancer. In addition, we have demonstrated a significant relation between *PIK3CA* G>A mutation and loss of MGMT expression. Because *MGMT* methylation or loss has been associated with G>A mutations of the *KRAS* and *TP53* genes [38,39], our findings could also attribute at least some *PIK3CA* G>A mutations in colorectal cancer to MGMT loss and subsequent DNA repair defect.

Our resource of a large population-based sample of colorectal cancer (relatively unbiased samples compared with retrospective or single-hospital–based samples), derived from two prospective cohorts, has enabled us to precisely estimate the frequency of a specific molecular event (such as *PIK3CA* mutation, CIMP-high, *KRAS* mutation, etc.). In fact, distribution and frequencies of various *PIK3CA* mutations in our sample are compatible with data in the previous studies [8–13].

Analysis of molecular alterations has been important in cancer research [40–49]. We used Pyrosequencing technology that has been shown to be more sensitive than regular Sanger sequencing in *KRAS* mutation analysis [22]. Pyrosequencing is nonelectrophoretic sequencing by nucleotide extension and is particularly useful for the analysis of single nucleotide polymorphisms or hotspot mutations in neoplasias [22]. Pyrosequencing assay for *PIK3CA* mutation detection is certainly useful, because most activating *PIK3CA* mutations cluster in hotspots of exons 9 and 20, affecting the functionally important helical and kinase domains [8,41].

The relationship between *PIK3CA* mutation and MSI in colorectal cancer has been examined in previous studies [9,11,13]; however, CIMP status has not been examined in these studies. We have shown that *PIK3CA* mutation is significantly associated with CIMP-high but not with MSI. Because there is a strong association between MSI-high and CIMP-high [16–18], the association of MSI with *PIK3CA* mutations in the previous report [11] might be due to the enrichment of CIMP-high tumors among MSI-high tumors. Analyzing both MSI and CIMP status has increasing importance in colorectal cancer research, because MSI and CIMP reflect global genomic and epigenomic aberrations in tumor cells, and largely determine clinical, pathologic, and molecular features of colorectal cancer [20,21].

Previous studies on colorectal cancer have shown the association between *PIK3CA* and *KRAS* mutations [13] or that between *PIK3CA* mutation and the presence of either *KRAS* or *BRAF* mutation [9]. However, other studies failed to demonstrate a significant relation between *PIK3CA* and *KRAS* mutations in colorectal cancer [10–12]. Using a large number of colorectal cancers, we confirmed the significant association between *PIK3CA* and *KRAS* mutations. The positive correlation between *PIK3CA* and *KRAS* mutations may suggest a synergistic effect of *PIK3CA* and *KRAS* mutations in activating the PI3K-AKT pathway during colorectal cancer development. We have also shown that *PIK3CA* mutation is associated with the expression of phospho-RPS6, downstream of the AKT and *FRAP1* (mTOR) pathways.

Our data indicate that *PIK3CA* mutation is associated with FASN expression, supporting the role of the PI3K-AKT pathway in the regulation of FASN expression [43,45]. FASN over-expression has been reported to be associated with AKT activation in various cancers [5,6,43]. However, no previous study has examined the relation between FASN expression and *PIK3CA* mutation in colorectal cancer. The PI3K-AKT pathway has been known to mediate signals from growth factors that are influenced by the state of energy balance [1,2], and FASN is also regulated by the altered energy balance in cells through AMP-dependent kinase [50,51]. Taken together, the PI3K-AKT pathway and FASN may indeed link altered energy balance and pathogenesis of neoplasia.

PIK3CA mutation has been associated with poor prognosis in colorectal cancer, although there were only 18 *PIK3CA*-mutated tumors [10]. Larger studies are necessary to confirm the association between *PIK3CA* mutation and poor outcome. A large population-based study has shown that a combination of *PIK3CA*, *KRAS*, and *BRAF* mutations predicts poor outcome in colon cancer [13]. Again, these results need to be confirmed by independent data sets.

In conclusion, using a large number of population-based colorectal cancers, we have demonstrated that *PIK3CA* mutation is significantly associated with *KRAS* mutation, CIMP-high, and FASN expression and inversely with p53 and β-catenin alterations. Pyrosequencing technology has proven to be a useful method in detecting *PIK3CA* mutation in a paraffin-embedded tumor tissue. In addition, loss of MGMT expression may play a role in the development of *PIK3CA* G>A mutation. *PIK3CA* mutational data by us and others further emphasize heterogeneity of colorectal cancer at the molecular level.

Acknowledgments

The authors deeply thank the Nurses' Health Study and Health Professionals Follow-up Study cohort participants who have generously agreed to provide us with biologic specimens and information through responses to questionnaires. The authors thank Walter Willett, Sue Hankinson, and many other staff members who implemented and have maintained the cohort studies.

Conflicts of interest: L. Y. is an employee of EpigenDx that provides service related to Pyrosequencing technology. No other conflict of interest is present.

References

[1] Manning BD and Cantley LC (2007). AKT/PKB signaling: navigating downstream. *Cell* **129**, 1261–1274.

[2] Engelman JA, Luo J, and Cantley LC (2006). The evolution of phosphatidylinositol 3-kinases as regulators of growth and metabolism. *Nat Rev Genet* **7**, 606–619.

[3] Samuels Y and Velculescu VE (2004). Oncogenic mutations of *PIK3CA* in human cancers. *Cell Cycle* **3**, 1221–1224.

[4] Yang YA, Han WF, Morin PJ, Chrest FJ, and Pizer ES (2002). Activation of fatty acid synthesis during neoplastic transformation: role of mitogen-activated protein kinase and phosphatidylinositol 3-kinase. *Exp Cell Res* **279**, 80–90.

[5] Van de Sande T, Roskams T, Lerut E, Joniau S, Van Poppel H, Verhoeven G, and Swinnen JV (2005). High-level expression of fatty acid synthase in human prostate cancer tissues is linked to activation and nuclear localization of Akt/PKB. *J Pathol* **206**, 214–219.

[6] Wang HQ, Altomare DA, Skele KL, Poulikakos PI, Kuhajda FP, Di Cristofano A, and Testa JR (2005). Positive feedback regulation between AKT activation and fatty acid synthase expression in ovarian carcinoma cells. *Oncogene* **24**, 3574–3582.

[7] Kuhajda FP (2006). Fatty acid synthase and cancer: new application of an old pathway. *Cancer Res* **66**, 5977–5980.

[8] Samuels Y, Wang Z, Bardelli A, Silliman N, Ptak J, Szabo S, Yan H, Gazdar A, Powell SM, Riggins GJ, et al. (2004). High frequency of mutations of the *PIK3CA* gene in human cancers. *Science* **304**, 554.

[9] Velho S, Oliveira C, Ferreira A, Ferreira AC, Suriano G, Schwartz S Jr, Duval A, Carneiro F, Machado JC, Hamelin R, et al. (2005). The prevalence of *PIK3CA* mutations in gastric and colon cancer. *Eur J Cancer* **41**, 1649–1654.

[10] Kato S, Iida S, Higuchi T, Ishikawa T, Takagi Y, Yasuno M, Enomoto M, Uetake H, and Sugihara K (2007). *PIK3CA* mutation is predictive of poor survival in patients with colorectal cancer. *Int J Cancer* **121**, 1771–1778.

[11] Abubaker J, Bavi P, Al-Harbi S, Ibrahim M, Siraj AK, Al-Sanea N, Abduljabbar A, Ashari LH, Alhomoud S, Al-Dayel F, et al. (2008). Clinicopathological analysis of colorectal cancers with *PIK3CA* mutations in Middle Eastern population. *Oncogene* (Epub ahead of print).

[12] Benvenuti S, Frattini M, Arena S, Zanon C, Cappelletti V, Coradini D, Daidone MG, Pilotti S, Pierotti MA, and Bardelli A (2008). *PIK3CA* cancer mutations display gender and tissue specificity patterns. *Hum Mutat* **29**, 284–288.

[13] Barault L, Veyries N, Jooste V, Lecorre D, Chapusot C, Ferraz JM, Lievre A, Cortet M, Bouvier AM, Rat P, et al. (2008). Mutations in the RAS-MAPK, PI(3)K (phosphatidylinositol-3-OH kinase) signaling network correlate with poor survival in a population-based series of colon cancers. *Int J Cancer* **122**, 2255–2259.

[14] Miyaki M, Iijima T, Yamaguchi T, Takahashi K, Matsumoto H, Yasutome M, Funata N, and Mori T (2007). Mutations of the *PIK3CA* gene in hereditary colorectal cancers. *Int J Cancer* **121**, 1627–1630.

[15] Ollikainen M, Gylling A, Puputti M, Nupponen NN, Abdel-Rahman WM, Butzow R, and Peltomaki P (2007). Patterns of *PIK3CA* alterations in familial colorectal and endometrial carcinoma. *Int J Cancer* **121**, 915–920.

[16] Samowitz W, Albertsen H, Herrick J, Levin TR, Sweeney C, Murtaugh MA, Wolff RK, and Slattery ML (2005). Evaluation of a large, population-based sample supports a CpG island methylator phenotype in colon cancer. *Gastroenterology* **129**, 837–845.

[17] Ogino S, Cantor M, Kawasaki T, Brahmandam M, Kirkner G, Weisenberger DJ, Campan M, Laird PW, Loda M, and Fuchs CS (2006). CpG island methylator phenotype (CIMP) of colorectal cancer is best characterised by quantitative DNA methylation analysis and prospective cohort studies. *Gut* **55**, 1000–1006.

[18] Weisenberger DJ, Siegmund KD, Campan M, Young J, Long TI, Faasse MA, Kang GH, Widschwendter M, Weener D, Buchanan D, et al. (2006). CpG island methylator phenotype underlies sporadic microsatellite instability and is tightly associated with *BRAF* mutation in colorectal cancer. *Nat Genet* **38**, 787–793.

[19] Grady WM (2007). CIMP and colon cancer gets more complicated. *Gut* **56**, 1498–1500.

[20] Ogino S and Goel A (2008). Molecular classification and correlates in colorectal cancer. *J Mol Diagn* **10**, 13–27.

[21] Jass JR (2007). Classification of colorectal cancer based on correlation of clinical, morphological and molecular features. *Histopathology* **50**, 113–130.

[22] Ogino S, Kawasaki T, Brahmandam M, Yan L, Cantor M, Namgyal C, Mino-Kenudson M, Lauwers GY, Loda M, and Fuchs CS (2005). Sensitive sequencing method for *KRAS* mutation detection by Pyrosequencing. *J Mol Diagn* **7**, 413–421.

[23] Colditz GA and Hankinson SE (2005). The Nurses' Health Study: lifestyle and health among women. *Nat Rev Cancer* **5**, 388–396.

[24] Giovannucci E, Liu Y, Rimm EB, Hollis BW, Fuchs CS, Stampfer MJ, and Willett WC (2006). Prospective study of predictors of vitamin D status and cancer incidence and mortality in men. *J Natl Cancer Inst* **98**, 451–459.

[25] Chan AT, Ogino S, and Fuchs CS (2007). Aspirin and the risk of colorectal cancer in relation to the expression of COX-2. *N Engl J Med* **356**, 2131–2142.

[26] Ogino S, Kawasaki T, Kirkner GJ, Kraft P, Loda M, and Fuchs CS (2007). Evaluation of markers for CpG island methylator phenotype (CIMP) in colorectal cancer by a large population-based sample. *J Mol Diagn* **9**, 305–314.

[27] Dietmaier W, Hartmann A, Wallinger S, Heinmoller E, Kerner T, Endl E, Jauch KW, Hofstadter F, and Ruschoff J (1999). Multiple mutation analyses in single tumor cells with improved whole genome amplification. *Am J Pathol* **154**, 83–95.

[28] Ogino S, Kawasaki T, Kirkner GJ, Loda M, and Fuchs CS (2006). CpG island methylator phenotype-low (CIMP-low) in colorectal cancer: possible associations with male sex and *KRAS* mutations. *J Mol Diagn* **8**, 582–588.

[29] Ogino S, Brahmandam M, Cantor M, Namgyal C, Kawasaki T, Kirkner G, Meyerhardt JA, Loda M, and Fuchs CS (2006). Distinct molecular features of colorectal carcinoma with signet ring cell component and colorectal carcinoma with mucinous component. *Mod Pathol* **19**, 59–68.

[30] Boland CR, Thibodeau SN, Hamilton SR, Sidransky D, Eshleman JR, Burt RW, Meltzer SJ, Rodriguez-Bigas MA, Fodde R, Ranzani GN, et al. (1998). A National Cancer Institute Workshop on Microsatellite Instability for cancer detection and familial predisposition: development of international criteria for the determination of microsatellite instability in colorectal cancer. *Cancer Res* **58**, 5248–5257.

[31] Eads CA, Danenberg KD, Kawakami K, Saltz LB, Blake C, Shibata D, Danenberg PV, and Laird PW (2000). MethyLight: a high-throughput assay to measure DNA methylation. *Nucleic Acids Res* **28**, E32.

[32] Ogino S, Kawasaki T, Brahmandam M, Cantor M, Kirkner GJ, Spiegelman D, Makrigiorgos GM, Weisenberger DJ, Laird PW, Loda M, et al. (2006). Precision and performance characteristics of bisulfite conversion and real-time PCR (MethyLight) for quantitative DNA methylation analysis. *J Mol Diagn* **8**, 209–217.

[33] Kawasaki T, Nosho K, Ohnishi M, Suemoto Y, Kirkner GJ, Fuchs CS, and Ogino S (2007). IGFBP3 promoter methylation in colorectal cancer: relationship with microsatellite instability, CpG island methylator phenotype (CIMP) and p53. *Neoplasia* **9**, 1091–1098.

[34] Ogino S, Brahmandam M, Kawasaki T, Kirkner GJ, Loda M, and Fuchs CS (2006). Combined analysis of COX-2 and p53 expressions reveals synergistic inverse correlations with microsatellite instability and CpG island methylator phenotype in colorectal cancer. *Neoplasia* **8**, 458–464.

[35] Ogino S, Kawasaki T, Kirkner GJ, Suemoto Y, Meyerhardt JA, and Fuchs CS (2007). Molecular correlates with MGMT promoter methylation and silencing support CpG island methylator phenotype–low (CIMP-low) in colorectal cancer. *Gut* **56**, 1409–1416.

[36] Kawasaki T, Nosho K, Ohnishi M, Suemoto Y, Kirkner GJ, Dehari R, Meyerhardt JA, Fuchs CS, and Ogino S (2007). Correlation of beta-catenin localization with cyclooxygenase-2 expression and CpG island methylator phenotype (CIMP) in colorectal cancer. *Neoplasia* **9**, 569–577.

[37] Jass JR, Biden KG, Cummings MC, Simms LA, Walsh M, Schoch E, Meltzer SJ, Wright C, Searle J, Young J, et al. (1999). Characterisation of a subtype of colorectal cancer combining features of the suppressor and mild mutator pathways. *J Clin Pathol* **52**, 455–460.

[38] Esteller M, Risques RA, Toyota M, Capella G, Moreno V, Peinado MA, Baylin SB, and Herman JG (2001). Promoter hypermethylation of the DNA repair gene *O*(6)-methylguanine-DNA methyltransferase is associated with the presence of G:C to A:T transition mutations in p53 in human colorectal tumorigenesis. *Cancer Res* **61**, 4689–4692.

[39] Esteller M, Toyota M, Sanchez-Cespedes M, Capella G, Peinado MA, Watkins DN, Issa JP, Sidransky D, Baylin SB, and Herman JG (2000). Inactivation of the DNA repair gene O_6-methylguanine-DNA methyltransferase by promoter hypermethylation is associated with G to A mutations in K-*ras* in colorectal tumorigenesis. *Cancer Res* **60**, 2368–2371.

[40] Cengel KA, Voong KR, Chandrasekaran S, Maggiorella L, Brunner TB, Stanbridge E, Kao GD, McKenna WG, and Bernhard EJ (2007). Oncogenic K-*Ras* signals through epidermal growth factor receptor and wild-type H-*Ras* to promote radiation survival in pancreatic and colorectal carcinoma cells. *Neoplasia* **9**, 341–348.

[41] Ikenoue T, Kanai F, Hikiba Y, Obata T, Tanaka Y, Imamura J, Ohta M, Jazag A, Guleng B, Tateishi K, et al. (2005). Functional analysis of *PIK3CA* gene mutations in human colorectal cancer. *Cancer Res* **65**, 4562–4567.

[42] Tsareva SA, Moriggl R, Corvinus FM, Wiederanders B, Schutz A, Kovacic B, and Friedrich K (2007). Signal transducer and activator of transcription 3 activation promotes invasive growth of colon carcinomas through matrix metalloproteinase induction. *Neoplasia* **9**, 279–291.

[43] Chiang CT, Way TD, Tsai SJ, and Lin JK (2007). Diosgenin, a naturally occurring steroid, suppresses fatty acid synthase expression in HER2-overexpressing breast cancer cells through modulating Akt, mTOR and JNK phosphorylation. *FEBS Lett* **581**, 5735–5742.

[44] Derouet M, Wu X, May L, Hoon Yoo B, Sasazuki T, Shirasawa S, Rak J, and Rosen KV (2007). Acquisition of anoikis resistance promotes the emergence of oncogenic K-*ras* mutations in colorectal cancer cells and stimulates their tumorigenicity *in vivo*. *Neoplasia* **9**, 536–545.

[45] Porstmann T, Griffiths B, Chung YL, Delpuech O, Griffiths JR, Downward J, and Schulze A (2005). PKB/Akt induces transcription of enzymes involved in cholesterol and fatty acid biosynthesis via activation of SREBP. *Oncogene* **24**, 6465–6481.

[46] Barraclough J, Hodgkinson C, Hogg A, Dive C, and Welman A (2007). Increases in c-Yes expression level and activity promote motility but not proliferation of human colorectal carcinoma cells. *Neoplasia* **9**, 745–754.

[47] Kollmar O, Rupertus K, Scheuer C, Junker B, Tilton B, Schilling MK, and Menger MD (2007). Stromal cell–derived factor-1 promotes cell migration and tumor growth of colorectal metastasis. *Neoplasia* **9**, 862–870.

[48] Sasaki T, Kitadai Y, Nakamura T, Kim JS, Tsan RZ, Kuwai T, Langley RR, Fan D, Kim SJ, and Fidler IJ (2007). Inhibition of epidermal growth factor receptor and vascular endothelial growth factor receptor phosphorylation on tumor-associated endothelial cells leads to treatment of orthotopic human colon cancer in nude mice. *Neoplasia* **9**, 1066–1077.

[49] Henkhaus RS, Roy UK, Cavallo-Medved D, Sloane BF, Gerner EW, and Ignatenko NA (2008). Caveolin-1–mediated expression and secretion of kallikrein 6 in colon cancer cells. *Neoplasia* **10**, 140–148.

[50] Motoshima H, Goldstein BJ, Igata M, and Araki E (2006). AMPK and cell proliferation–AMPK as a therapeutic target for atherosclerosis and cancer. *J Physiol* **574**, 63–71.

[51] Menendez JA and Lupu R (2007). Fatty acid synthase and the lipogenic phenotype in cancer pathogenesis. *Nat Rev Cancer* **7**, 763–777.